Wireless Energy Harvesting Assisted Two-Way Cognitive Relay Networks

Protocol Design and Performance Analysis

Nguyen, Dang Khoa; Jayakody, Dushantha Nalin K.; Chatzinotas, Symeon; Thompson, John S.; Li, Jun

Published in:
IEEE Access

DOI (link to publication from Publisher):
10.1109/ACCESS.2016.2644758

Publication date:
2017

Document Version
Publisher's PDF, also known as Version of record

IEEE Access
Multidisciplinary | Rapid Review | Open Access Journal

Received November 23, 2016; accepted December 9, 2016, date of publication January 27, 2017,
date of current version October 25, 2017.

Digital Object Identifier 10.1109/ACCESS.2016.2644758

Wireless Energy Harvesting Assisted Two-Way Cognitive Relay Networks: Protocol Design and Performance Analysis

**DANG KHOA NGUYEN[1], (Student Member, IEEE),
DUSHANTHA NALIN K. JAYAKODY[2], (Member, IEEE),
SYMEON CHATZINOTAS[3], (Senior Member, IEEE)
JOHN S. THOMPSON[4], (Fellow, IEEE), AND JUN LI[5], (Senior Member, IEEE)**

[1]Department of Electronics System, Aalborg University, 9100 Aalborg, Denmark
[2]Department of Software Engineering, Institute of Cybernetics, National Research Tomsk Polytechnic University, Tomsk 634034, Russia
[3]Interdisciplinary Centre for Security, Reliability and Trust, University of Luxembourg, EH9 3JL Edinburgh, Luxembourg
[4]Institute for Digital Communications, School of Engineering, University of Edinburgh, Edinburgh EH8 9YL, U.K.
[5]Nanjing University of Science and Technology, Nanjing, China and he is also with National Mobile Communications Research Laboratory, Southeast University, Nanjing 210018, China

Corresponding author: Jun Li (jun.li@njust.edu.cn)

This work is supported in part by the National Natural Science Foundation of China under Grant 61501238, in part by the Jiangsu Provincial Science Foundation under Project BK20150786, in part by the Specially Appointed Professor Program in Jiangsu Province, 2015, in part by the Fundamental Research Funds for the Central Universities under Grant 30916011205, in part by the Open Research Fund of National Mobile Communications Research Laboratory, in part by the Southeast University under Grant 2017D04, in part by the Russian Federal Budget Funds under Grant 3942 and performed in accordance under Resolution 2014/226 of 2016, and in part by the Shared Access Terrestrial-Satellite Backhaul Network enabled by Smart Antennas H2020 framework under Grant 645047.

ABSTRACT This paper analyzes the effects of realistic relay transceiver on the outage probability and throughput of a two-way relay cognitive network that is equipped with an energy-harvesting relay. In this paper, we configure the network with two wireless power transfer policies and two bidirectional relaying protocols. Furthermore, the differences in receiver structure of relay node that can be time switching or power splitting structure are also considered to develop closed-form expressions of outage and throughput of the network providing that the delay of transmission is limited. Numerical results are presented to corroborate our analysis for all considered network configurations. This paper facilitates us not only to quantify the degradation of outage probability and throughput due to the impairments of realistic transceiver but also to provide an insight into practical effects of specified configuration of power transfer policy, relaying protocol, and receiver structure on outage and throughput. For instance, the system with multiple access broadcast protocol and the power splitting-based receiver architecture achieves ceiling throughout higher than that of the transmission rate of source nodes. On the contrary, a combination of dual-source energy transfer policy and the time division broadcast protocol is contributed the highest level of limiting factor in terms of transceiver hardware impairments on the network throughput.

INDEX TERMS Two-way relay, decode-and-forward, cognitive networks, energy harvesting, hardware impairments.

I. INTRODUCTION

As a sustainable solution to uphold the lifetime of energy constrained wireless networks, energy harvesting (EH) technique has recently received significant attention since it meets the requirements of green communications. Besides to the traditional renewable energy sources such as solar and wind, radio frequency (RF) signals radiated by ambient transmitters can be identified as a viable new inspiration for energy harvesting. In [1]–[3], wireless nodes acquire energy of RF signals in the surrounding environment to self-power the transmission data. Recently, some important advances of wireless power technologies have largely increased the feasibility of EH in practical wireless applications [4]–[6]. With concurrent developments in the antenna technology and EH circuit designs, wireless energy transfer is recognized as a valuable candidate for future networks.

Cognitive radio is emerging as a means to improve the wireless spectrum utilization [19]. In cognitive radio, secondary users (SUs) are allowed to transmit wireless signals in the same frequency bands that are officially allocated to primary users (PUs). In order to maintain quality-of-service of primary transmission links, the transmit power of SUs should be limited to the maximum interference allowance of PUs. Consequently, this power constraint limits the performance of SUs. In order to tackle the transmit power limitation in cognitive networks, the concept of two-way cognitive relay (TWCR) networks has been proposed in [8] and [9] among others. TWCR networks exploit the advantages of two-way relaying protocol and cognitive radio concepts. Also, they are able to overcome transmit power limitations and boost the system performance.

In the previous literature, the TWCR networks were analyzed using the outage probability (OP) and throughput of the systems under perfect transceiver hardware assumption, however this is far from the reality. In [8], a tight approximation of the OP for amplify-and-forward TWCR networks was provided.Closed-form expressions for the OP of TWCR network, in the presence of multiple primary users, were derived in [9]. However, transceivers in wireless communication system suffer from several types of impairments such as, in-phase/quadrature imbalance [10]–[12], and high power amplifier non-linearities [13]. Undoubtedly, transceiver impairments degrade the system performance, especially when the power budget is high [14]–[16].

Recent advances in opportunistic communications (OC) is possible to employee in interference alignment areas of wireless networks to improve the SINR performance. In [27], authors described novel SWIPT scheme based on opportunistic communications together with interference alignment. It is appeared that the research work on interference alignment has not focused attention to use interferences as useful resource for wireless RF energy harvesting. Authors in [27] and [29], re-utilizing the interferences as a constructive resource for powering the device. An adaptive power allocation scheme for interference alignment technique together with spectrum sharing is developed in [29]. In practice, one need to concern about the circuit power consumption when we computing the full energy usage account. In [30], maximizes the system energy efficiency while guaranteeing the user's quality of service via joint time allocation and power control. Maximization of energy transfer efficiency is an important step, in [31] and [32] maximizes the weighted sum of the user energy efficiencies for multi user scenario. In [33], discussed the distributing cellular data via a wireless power transfer enabled collaborative mobile cloud (WeCMC) in an energy efficient way. By use of device to device communication it cooperate with other users and offload the data from base station to other nodes. Similarly, minimizing the energy cost of data transmission in the context of orthogonal frequency-division multiple-access (OFDMA) collaborative mobile clouds (CMCs) with simultaneous wireless information and power transfer receivers is discussed in [34] and [35].

Cooperative diversity [6], [17] has been proposed as an effective approach to combat the fading effect and enhance channel throughput. In the literature, many research works have been conceived on cooperative relay techniques in cognitive radio for spectrum efficiency enhancement. In [6] and [7], the cooperative spectrum sensing techniques are used to enhance the reliability of detecting PUs in cognitive radio, and a cognitive space-time-frequency coding technique has been presented to adjust its coding structure by adapting itself to the dynamic spectrum environment. In specific applications such as wireless sensor networks in remote areas, where the power supply unit is difficult to recharge, a self-powered relay node is much preferable. Among various resources that can be converted to power, radio frequency energy is a preferred method in wireless networks. Hence, the relay nodes are able to be powered by the radio signals. However, the relevant research on the OP and throughput of radio frequency energy harvesting (EH) relaying has also assumed perfect hardware (see e.g., [20], [21], and references therein).

In this work, we present a detailed performance analysis of an EH based decode-and-forward (DF) TWCR network (EH-TWCR) in the presence of transceiver imperfections by utilizing the generalized impairment model of [22]. The main contributions of this paper are twofold:

1) We portray the self-powered EF-TWCR networks with two energy transfer policies, two relaying protocols, and two relay receiver structures while keeping the limited transmit power levels. To further explore the benefit on network throughput, we propose different data frame structures for the network with various combination of energy transfer policies, relaying protocols, and relay receiver architecture possible network cases with respect to the balanced comparison.
2) We provide new closed-form expressions for the OP and throughout of the considered networks under the impact of transceiver imperfection. Also, the influence of configuration parameters on network throughput is accounted. Our analysis set useful design guidelines for implementing a suitable protocol for EH-TWCR networks. Based on these results, network designers will be able to predict the maximum level of hardware imperfections that can be tolerated to achieve a predetermined performance.

This paper is organized as follows. Section II describes system configuration and channel model of a half-duplex TWCR network. In Section III, protocols of information and power transfer designed for the EH assisted DF-TWCR networks are explained. Section IV characterizes performance of time switching based architecture networks; whereas, section V discusses that of power splitting based architecture networks. Section VI is provided to validate our analytical model presented in the previous two section; and presents some useful results pertaining to system performance metrics. Section VII concludes this paper and explore future directions of the proposed network.

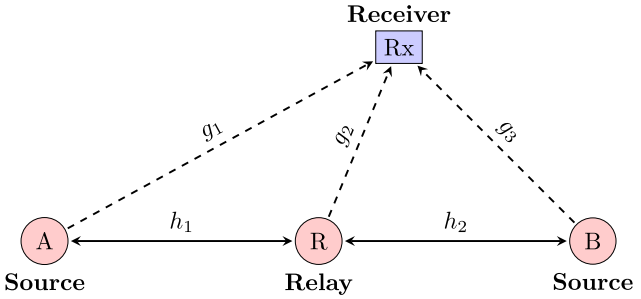

FIGURE 1. An energy harvesting two-way cognitive relay network.

II. SYSTEM AND CHANNEL MODEL

In this paper, we consider a half-duplex TWCR network as illustrated in Fig. 1. Primary user is the receiver (Rx), while the secondary users consists of two communication nodes A, B and one relay node R. Each node is equipped with a single antenna.

All channels of the cognitive relay network are assumed to be reciprocal and experience quasi-static block Rayleigh fading, whose coefficients are constant over the communication cycle T [21], [25], [26], [36]. The channel coefficients of the wireless communication links $A \to R$, $R \to B$, $A \to Rx$, $B \to Rx$ and $R \to Rx$ are denoted as h_m and g_n, where $m \in \{1, 2\}$ and $n \in \{1, 2, 3\}$ are complex Gaussian distributed random variables with zero mean and variances $\frac{1}{\lambda_m}$, and $\frac{1}{\omega_n}$, respectively. The additive noise terms η_i, $i \in \{A, B, R\}$, have zero mean and variance N_0, $\eta_i \sim \mathcal{CN}(0, N_0)$. Moreover, it is assumed that there is no line-of-sight transmission link from A to B. In addition, the channel state information of all wireless channels of the two hop information links are assumed to be known at the respective transmitter and receiver, which, for instance, could be obtained through feedback from a given node.

In order to protect the primary receiver (Rx) from secondary user interference signals, we define I_P as the maximum tolerance interference received at Rx to constrain the transmit powers of SUs. Thus, the peak transmit power is $P_i = \frac{I_P}{|g_n|^2}$ where $i \in \{A, B, R\}$ and $n \in \{1, 2, 3\}$. For our analysis, we determine the exponentially distributed random variables $\rho_m = |h_m|^2$, and $\nu_n = |g_n|^2$ for $m \in \{1, 2\}$ and $n \in \{1, 2, 3\}$, whose means are $\frac{1}{\lambda_m}$ and $\frac{1}{\omega_n}$, respectively. Finally, following the discussion in previous section, the aggregate impairment level during the information processing (IP) phase is represented by κ_i^2 where $i \in \{A, B, R\}$.

A. MODEL RECEIVED SIGNAL WITH IMPERFECTION TRANSCEIVER

In this paper, we modify the transceiver hardware impairments model originally in [22] to propose an unified model that can address hardware impairments generally. At first, assuming that a source transmits signal $x \in \mathbb{C}$ with power P_x over the wireless channel with fading coefficient h to the sink. Providing that the transmitted signal experiences AWGN η. In reality, signal x carries distortions that caused by imperfect transceivers at the source and sink. Each distortion is modeled as independent random variable. Yet, let τ_1, τ_2 be the *transceiver distortion* at the source and sink, respectively. The received signal can be succinctly expressed as

$$y = h(x + \tau_1) + \tau_2 + \eta. \tag{1}$$

where $\tau_1 \sim \mathcal{CN}(0, \kappa_1^2 P_x)$ and $\tau_2 \sim \mathcal{CN}(0, \kappa_2^2 P_x |h|^2)$, where κ_1, κ_2 are the *impairment levels* of source and sink transceiver, respectively [23], [24]. By rearranging and simplifying (1), we have

$$y = hx + h\kappa_1^2 P_x + h\kappa_2^2 P_x + \eta = h(x + \tau) + \eta. \tag{2}$$

In (2), $\tau \sim \mathcal{CN}(0, \kappa^2 P_x)$ represents *end-to-end distortion* of a transmission from the source to sink of which transceivers are imperfection. Furthermore, $\kappa = \sqrt{\kappa_1^2 + \kappa_2^2}$ indicates *end-to-end impairment level* that covers impairment level at the source and sink. Hence, equation (2) can be used to address the impact of transceiver hardware impairments on the received signal.

III. DF-TWCR NETWORKS WITH ENERGY HARVESTING

In this section, we describe in detail our proposed transmission protocol in a EH-TWRC network, where information exchanged from two source nodes A and B is assisted by a self-powered intermediate node R. One transmission cycle is divided into three phases, energy harvesting phase and broadcast (BC) phase and relaying (RL) phase. The relay R harvests energy from wireless signals that transmitted from A (and B) in EH phase. Exchanged data from A and B are transmitted to R during BC phase. Then ar R, this received data is decoded and re-encoded with a implemented network coding scheme before forwarding to B and A in RL phase. Within this context, we configure the EH-TWCR network with two EH policies, dual-source (DS) and single-fixed-source (SFS) policy; two relaying protocols, time division broadcast (TDBC) and multiple access broadcast (MABC) protocol; and two relay receiver structures time switching based (TSB) and power splitting based (PSB) architecture.

We propose a paradigm that duration of the EH, and RL phase are fixed over the network configurations as $2t$, and t [sec], respectively, whereas, the duration of BC phase varies due to the network configuration (length $2t$ or t). Depending on the network configurations, the EH, BC and RL phase are contributed to form a transmission cycle, T. Thereby, the duration T varies corresponding to the network configuration. This paper presents the benefit of each network configuration and offer the balanced comparison on the performance between all possible network configurations. For the sake of convenience, we shorten the description of specific network configuration, for example, the network that is configured with DS energy transfer policy, TDBC relaying protocol, and TSB relay receiver architecture is denominated by DS-TDBC-TSB network. All possible network configurations are explained and analysed in the later parts of this paper.

A. ENERGY TRANSFER POLICY

During the EH phase, R harvests energy from the RF signals which are transmitted from other nodes in TWCR network. We assume that the transmit powers at A and (or) B to R in the EH phase satisfy the maximum allowable interference[1] I_P, hence $P_A^{EH} = P_B^{EH} = \widetilde{I}_P < \min\left(\frac{I_P}{\nu_1}, \frac{I_P}{\nu_3}\right)$. The collected energy at R is utilized to decode and re-encode data in BC phase and also transmit signal in the RL phase. The amount of harvested power depends on energy transfer policy, the power conversion efficiency of the rectification circuit and the receiver architecture of relay node. The power conversion efficiency is denoted as μ $(0 < \mu \leq 1)$ [25]. Note that hardware impairments are not taken into account during the EH phase as (a) the hardware used for harvesting energy is different from that used in transmitting/receiving data, and (b) any type of hardware imperfections in the EH circuitry is eventually captured by μ. Two energy transfer policies, i.e., DS and SFS policy, are described in the following section.

1) DS ENERGY TRANSFER POLICY

In the DS energy transfer policy, the relay harvests power from the signals that are transmitted from both A and B during the EH phase.

2) SFS ENERGY TRANSFER POLICY

In this policy, the relay harvests power from the transmitted signal either A or B which is predetermined before transmission take place. Without loss of generality, the received signal in EH phase at R for the SFS policy is assumed to be transmitted from the fixed node A.

B. RELAYING PROTOCOL

In this section, we describe two relaying protocols: the TDBC and MABC. The relay protocols consist of two data transmission phases, i.e., BC and RL phase. The frame structure of the BC phase determines the category of relaying protocol. Note that the decoders and encoders of each node in TWCR network are assumed to be flawless.

1) TDBC PROTOCOL

In the TDBC protocol, the duration of BC phase is divided into two equal time slots (length of durations are equal to half of the BC phase). In the first time slot, A transmits signal to R, whereas B transmits to R in the second time slot. The received data at R is decoded and re-encoded, then it is combined with XOR operation (network coding) before forwarded to B and A in the RL phase.

2) MABC PROTOCOL

In the MABC protocol, R concurrently receives data from both node A and node B via two orthogonal channels in the BC phase. The received data at R is also decoded, re-encoded then combined with XOR operation (network coding) before forwarded to B and A in the RL phase.

[1]The minimal RF input power required for sensor node operation was found to be -18 dBm (15.8 μW). Using a 6 dBm receive antenna, the most sensitive RF harvester was shown to operate at a distance of several kilometers from a 1 MW UHF television broadcast tower, and over 200 m from a cellular base transceiver station [37].

C. RELAY RECEIVER ARCHITECTURE

The architecture of relay receiver determines the strategy that data received from antenna of the relay is feed to its energy harvesting block and data processing block in chronology or concurrence. Therefore, the receiver architecture affects the frame structure and the length of T. In this paper, we consider two structures of relay receiver namely, TSB and PSB architectures [25].

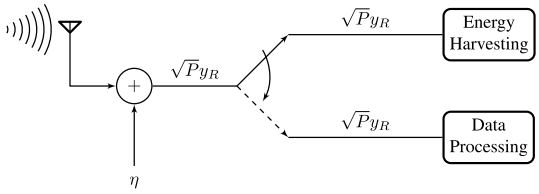

FIGURE 2. Relay receiver with TSB architecture.

1) TSB ARCHITECTURE

The TSB architecture is depicted in the Fig. 2. The receiver antenna of the relay is successively connected to the energy harvesting block and the data processing block over time. The incoming data to these blocks is controlled by the timing mechanism. Hence, the EH phase and the BC phase occur in two separated time slots.

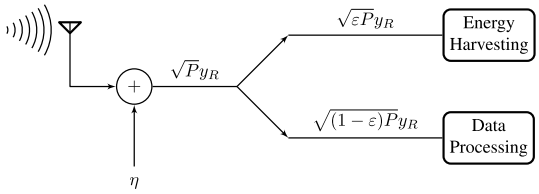

FIGURE 3. Relay receiver with PSB architecture.

2) PSB ARCHITECTURE

The PSB architecture is depicted in the Fig. 3. The receive antenna of the relay is connected to both energy harvesting block and data processing block. Therefore, the received data at the relay antenna is shared with these blocks. ε is defined as power sharing fraction $(0 < \varepsilon < 1)$. Due to this receiver structure, the EH phase and the BC phase may concurrently occur in a given time slot, the transmission cycle can therefore be shortened, thereof. This is a benefit offered by the PSB architecture over the TSB architecture.

IV. PERFORMANCE ANALYSIS: TSB ARCHITECTURE

In this section, we elaborate on the impact of transceiver impairments on the *signal to noise plus distortion ratio* (SNDR), the outage performance and throughput of the EH DF TWCR networks. The relay receiver is configured with TSB architecture.

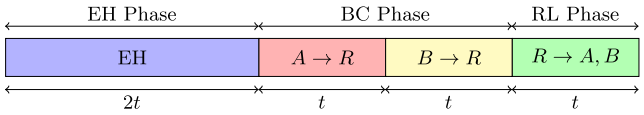

FIGURE 4. Data frame structure of the DS-TDBC-TSB network.

A. DS POLICY - TDBC PROTOCOL

In this configuration, the network utilizes the DS policy - TDBC protocol - TSB architecture. The data frame structure of the communication cycle T is shown in Fig. 4. The relay R harvests energy from transmitted signals from both A and B in the EH phase. Then, R consequently receive the transmit data from A and B in the first and the second time slot of the BC phase. Later, R forwards the re-encoded signal to both A and B in the RL phase. Thus, the duration of T is $5t$ [sec]. The acquired energy at R is parametrized as

$$E_H = \mu\left(P_A^{EH}|h_1|^2 + P_B^{EH}|h_2|^2\right)2t = \mu\widetilde{I}_P(\rho_1+\rho_2)2t. \quad (3)$$

1) TRANSMIT POWER IN THE RL PHASE

In order to determine the end-to-end SNDR, we need the information of transmit energy of the relay in the RL phase. The harvested energy in the EH phase is used for decoding, re-encoding signals in the BC phase as well as forwarding data in the RL phase. We assume that the total harvested energy at R in the EH phase is distributed equally to the total duration of the BC phase and the RL phase. Thus, from (3), the transmit power at R in the RL phase is

$$P_R = \frac{E_H}{3t} = \frac{\mu\widetilde{I}_P 2t}{3t}(\rho_1+\rho_2) = \Upsilon_1(\rho_1+\rho_2), \quad (4)$$

where $\Upsilon_1 = \frac{2}{3}\mu\widetilde{I}_P$.

2) END-TO-END SNDR

In the BC phase, the information transfers in different time slots from A and B to R, hence, the instantaneous SNDR at either R of the link $A \to R$ and $B \to R$ or at A (or at B) of the link $R \to A$ (or the link $R \to B$) in the RL phase, respectively, are independent and statistically similar. Without loss of generality, only the communication link $A \to R \to B$ is investigated herein. We assume that A transmits data with the peak power $\frac{I_P}{\nu_1}$. Then, the SNDR at R of the $A \to R$ link is given by

$$\gamma_1 = \frac{\frac{I_P}{N_0}|h_1|^2}{\frac{I_P}{N_0}\kappa_R^2|h_1|^2 + |g_1|^2} = \frac{\bar{\gamma}\rho_1}{\bar{\gamma}\kappa_R^2\rho_1 + \nu_1}, \quad (5)$$

where $\bar{\gamma} \triangleq \frac{I_P}{N_0}$. In the RL phase, R forwards the received data from the previous two time slots to A and B with the transmit power equals to $\frac{P_R}{\nu_2}$. P_R is given in (4). Then, the SNDR at B of the link $R \to B$ is given by

$$\gamma_2 = \frac{\bar{\Upsilon}_1(\rho_1+\rho_2)}{\bar{\Upsilon}_1\kappa_B^2(\rho_1+\rho_2) + \frac{\nu_2}{\rho_2}}, \quad (6)$$

where $\bar{\Upsilon}_1 = \frac{\Upsilon_1}{N_0}$. The end-to-end SNDR of the wireless link $A \to R \to B$ of is then obtained as

$$\gamma = \min(\gamma_1, \gamma_2). \quad (7)$$

3) OUTAGE PERFORMANCE ANALYSIS

Denote that $F(\cdot)$ and $f(\cdot)$ are the cumulative distributed function (CDF) and the probability distributed fucntion (PDF) of a random variable (RV), respectively. In (5) and (6), ρ_1 appears as a common RV in both γ_1 and γ_2, therefore the CDF of γ, $F_\gamma(\gamma)$, in (7) can be expressed as

$$F_\gamma(\gamma) = \int_0^\infty \Big[F_{\gamma_1|\rho_1}(\gamma) + F_{\gamma_2|\rho_1}(\gamma) - F_{\gamma_1|\rho_1}(\gamma)F_{\gamma_2|\rho_1}(\gamma)\Big]f_{\rho_1}(x)dx. \quad (8)$$

The following propositions will enable us to analytically evaluate (8).

Proposition 1: The CDF of γ_1 conditioned on ρ_1 is given by

$$F_{\gamma_1|\rho_1}(\gamma) = \exp\left(-\frac{\bar{\gamma}(1-\kappa_R^2\gamma)}{\omega_1\gamma}\rho_1\right). \quad (9)$$

Proof: From the definition of the CDF of a RV, we have

$$F_{\gamma_1|\rho_1}(\gamma) = \Pr\left[\frac{\bar{\gamma}\rho_1}{\bar{\gamma}\rho_1\kappa_R^2 + \nu_1} \le \gamma\right] = 1 - F_{\nu_1}\left(\frac{\bar{\gamma}(1-\kappa_R^2\gamma)\rho_1}{\gamma}\right).$$

This result leads directly to (9). ■

Proposition 2: The CDF of γ_2 conditioned on ρ_1 is given by

$$F_{\gamma_2|\rho_1}(\gamma) = \frac{\omega_2}{\lambda_2^2 C_1}\exp\left(\frac{\rho_1}{\lambda_2}\right)\exp\left(\frac{\omega_2}{\lambda_2^2 C_1}\right)\mathrm{E}_1\left(\frac{\omega_2}{\lambda_2^2 C_1}\right) \quad (10)$$

where $C_1 \triangleq \frac{\bar{\Upsilon}_1(1-\kappa_B^2\gamma)}{\gamma}$, and $\mathrm{E}_1(x) = \int_x^\infty \frac{\mathrm{e}^{-t}}{t}dt$ is the exponential integral function.

Proof: By the definition of CDF of a RV, we have

$$F_{\gamma_2|\rho_1}(\gamma) = \Pr\left[\frac{\bar{\Upsilon}_1(\rho_1+\rho_2)}{\bar{\Upsilon}_1\kappa_B^2(\rho_1+\rho_2) + \frac{\nu_2}{\rho_2}} \le \gamma\right] = 1 - \int_0^\infty F_X(C_1 y)f_{Y|\rho_1}(y)dy \quad (11)$$

where $X \triangleq \frac{\nu_2}{\rho_2}$ and $Y \triangleq \rho_1 + \rho_2$. It is apparent that $F_X(x) = 1 - \frac{\omega_2}{x\lambda_2+\omega_2}$ and $f_{Y|\rho_1}(y) = \frac{1}{\lambda_2}\exp\left(-\frac{y-\rho_1}{\lambda_2}\right)$. Substituting these results into (11), we obtain

$$F_{\gamma_2|\rho_1}(\gamma) = \int_0^\infty \left(\frac{\omega_2}{\omega_2+\lambda_2 y}\right)\frac{1}{\lambda_2}\exp\left(-\frac{y-\rho_1}{\lambda_2}\right)dy. \quad (12)$$

After some algebraic manipulations and using [38, eq. (3.352.4)], we can obtain the result shown in (10). ■

Using the previous theorems, (8) is recast as

$$F_\gamma(\gamma) = I_1 + I_2 - I_3, \tag{13}$$

where we can define from Proposition 1 and Proposition 2:

$$I_1 = \frac{\omega_1\gamma}{\omega_1\gamma + \lambda_1\bar{\gamma}(1-\kappa_R^2\gamma)},$$

$$I_2 = C_2\frac{\lambda_2}{\lambda_1+\lambda_2}, \quad C_2 \triangleq \frac{\omega_2}{\lambda_2^2 C_1}\exp\left(\frac{\omega_2}{\lambda_2^2 C_1}\right)\mathrm{E}_1\left(\frac{\omega_2}{\lambda_2^2 C_1}\right),$$

$$I_3 = C_2\frac{\lambda_2\omega_1}{\lambda_1\lambda_2\bar{\gamma}(1-\kappa_R^2\gamma)+\omega_1\gamma(\lambda_1+\lambda_2)}.$$

Gathering the previous results together, the OP at nodes A and B at a specific SNDR threshold (γ_t) of the networks is given in (14) and (15), respectively.

$$\begin{aligned} &OP_A(\gamma_t) \\ &= \frac{\omega_3\gamma_t}{\omega_3\gamma_t + \lambda_2\bar{\gamma}(1-\kappa_R^2\gamma_t)} + \frac{\omega_2}{\lambda_1^2 C_1}\exp\left(\frac{\omega_2}{\lambda_1^2 C_1}\right) \\ &\quad\times\mathrm{E}_1\left(\frac{\omega_2}{\lambda_1^2 C_1}\right)\left[\frac{\lambda_1}{\lambda_2+\lambda_1}\right. \\ &\quad\left.-\frac{\lambda_1\omega_3}{\lambda_2\lambda_1\bar{\gamma}(1-\kappa_R^2\gamma_t)+\omega_3\gamma_t(\lambda_2+\lambda_1)}\right]. \end{aligned} \tag{14}$$

$$\begin{aligned} &OP_B(\gamma_t) \\ &= \frac{\omega_1\gamma_t}{\omega_1\gamma_t + \lambda_1\bar{\gamma}(1-\kappa_R^2\gamma_t)} + \frac{\omega_2}{\lambda_2^2 C_1}\exp\left(\frac{\omega_2}{\lambda_2^2 C_1}\right) \\ &\quad\times\mathrm{E}_1\left(\frac{\omega_2}{\lambda_2^2 C_1}\right)\left[\frac{\lambda_2}{\lambda_1+\lambda_2}\right. \\ &\quad\left.-\frac{\lambda_2\omega_1}{\lambda_1\lambda_2\bar{\gamma}(1-\kappa_R^2\gamma_t)+\omega_1\gamma_t(\lambda_1+\lambda_2)}\right]. \end{aligned} \tag{15}$$

Outage probability of the DS-TDBC-TSB networks is the sum of the OP of the link $A \to R \to B$ and the OP of the link $B \to R \to A$. It is obtained as

$$OP(\gamma_t) = OP_A(\gamma_t) + OP_B(\gamma_t), \tag{16}$$

where $OP_A(\gamma_t)$ and $OP_B(\gamma_t)$ are the OP at A and B, given in 14 and 15, respectively.

4) THROUGHPUT ANALYSIS

We assume that the sources transmit information to the destinations at a fixed communication rate. We can now analyze the network throughput in the context of delay-limited transmission. The transmission rates at A and B of the TWCR networks are given as $R_A = \log_2(1+\gamma_A)$ and $R_B = \log_2(1+\gamma_B)$ [bits/s/Hz], respectively, where γ_A and γ_B are the corresponding threshold SNDRs. The network throughput is measured as the sum of the throughput of each wireless link at a given transmit rate. Hence, the network throughput, $\mathcal{T}$, in this network configuration is determined as

$$\mathcal{T} = \frac{t}{5}\Big[R_A(1-OP_A(\gamma_A)) + R_B(1-OP_B(\gamma_B))\Big], \tag{17}$$

where $OP_A(\gamma_A)$ and $OP_B(\gamma_B)$ are the OPs at A and B, respectively. By substituting the OPs at A and B from (14) and (15) into (17), the exact expression of the network throughput is obtained.

B. SFS POLICY - TDBC PROTOCOL

In this subsection, the network is configured with SFS policy, TDBC protocol, and utilizes TSB receiver architecture. The data frame structure of the transmission cycle T is similar to the one of DS-TDBC-TSB network that was shown in Fig. 4. The only different is R harvests energy from the signal that is transmitted from A only. The energy harvested at R is then given by

$$E_H = \mu P_A^{EH}|h_1|^2 2t = \mu\widetilde{I}_P\rho_1 2t. \tag{18}$$

1) TRANSMIT POWER IN THE RL PHASE

Similarly, we assume that the entire harvested energy at R in the EH phase is distributed equally to the total duration of BC phase and RL phase. Thus, from (18), the transmit power at R in the RL phase equals to

$$P_R = \frac{E_H}{3t} = \frac{\mu\widetilde{I}_P 2t}{3t}\rho_1 = \Upsilon_1\rho_1. \tag{19}$$

2) END-TO-END SNDR

As the transmit power at R is harvested from A, the SNDR of the link $A \to R \to B$ is different from the SNDR of the link $B \to R \to A$. Similarly, we assumed that A and B transmit data with peak power $\frac{I_P}{\nu_1}$ and $\frac{I_P}{\nu_3}$, respectively. The transmit power at R in the RL phase equals to $\frac{P_R}{\nu_2}$, P_R is the harvested energy at R that is given in (19). The SNDRs at R and B of the link $A \to R \to B$ are given respectively by

$$\gamma_{1,ARB} = \frac{\bar{\gamma}\rho_1}{\bar{\gamma}\kappa_R^2\rho_1 + \nu_1}, \tag{20}$$

$$\gamma_{2,ARB} = \frac{\bar{\Upsilon}_1\rho_1\rho_2}{\bar{\Upsilon}_1\kappa_B^2\rho_1\rho_2 + \nu_2}. \tag{21}$$

Therefore, the end-to-end SNDR at B can be obtained as

$$\gamma_B = \min(\gamma_{1,ARB}, \gamma_{2,ARB}). \tag{22}$$

Consider the link $B \to R \to A$ now, the SNDRs at R and A are respectively given by

$$\gamma_{1,BRA} = \frac{\bar{\gamma}\rho_2}{\bar{\gamma}\kappa_R^2\rho_2 + \nu_3}, \tag{23}$$

$$\gamma_{2,BRA} = \frac{\bar{\Upsilon}_1\rho_1}{\bar{\Upsilon}_1\kappa_A^2\rho_1 + \frac{\nu_2}{\rho_1}}. \tag{24}$$

Likewise, the end-to-end SNDR at A is calculated as

$$\gamma_A = \min(\gamma_{1,BRA}, \gamma_{2,BRA}). \tag{25}$$

3) OUTAGE PERFORMANCE ANALYSIS

It can be seen that ρ_1 appears as a common RV in both $\gamma_{1,ARB}$ and $\gamma_{2,ARB}$ as given in (20) and (21), respectively. Hence, the

end-to-end CDF γ_B needs to be computed as follows:

$$F_{\gamma_B}(\gamma) = \int_0^\infty \Big[F_{\gamma_{1,ARB}|\rho_1}(\gamma) + F_{\gamma_{2,ARB}|\rho_1}(\gamma) - F_{\gamma_{1,ARB}|\rho_1}(\gamma)F_{\gamma_{,ARB}|\rho_1}(\gamma)\Big]f_{\rho_1}(x)dx. \quad (26)$$

The following proposition will enable us to evaluate (26).

Proposition 3: The CDF of $\gamma_{2,ARB}$ conditioned on ρ_1 is given by

$$F_{\gamma_{2,ARB}|\rho_1}(\gamma) = \frac{\omega_2\gamma}{\omega_2\gamma + (1-k_B^2\gamma)\bar{\Upsilon}_1\lambda_2\rho_1}. \quad (27)$$

Proof: From the definition of the CDF of a RV, we have

$$F_{\gamma_{2,ARB}|\rho_1}(\gamma) = \Pr\left[\frac{\bar{\Upsilon}_1\rho_1\rho_2}{\bar{\Upsilon}_1\kappa_B^2\rho_1\rho_2 + \nu_2} < \gamma\right] = 1 - \int_0^\infty F_{\nu_2}\left(\frac{\bar{\Upsilon}_1(1-\kappa_B^2\gamma)\rho_1 x}{\gamma}\right)f_{\rho_2}(x)dx.$$

By substituting CDF and PDF of the exponential RV ρ_2 into the above equation, the CDF of $\gamma_{2,ARB}$ conditioned on ρ_1 can be obtained as in (27). ■

The CDF of $\gamma_{1,ARB}$ conditioned on ρ_1 can be obtained with the help of Proposition 1. In particular, we can readily show that

$$F_{\gamma_{1,ARB}|\rho_1}(\gamma) = \exp\left(-\frac{\bar{\gamma}(1-\kappa_R^2\gamma)\rho_1}{\omega_1\gamma}\right). \quad (28)$$

The end-to-end CDF of γ_B is derived by substituting (26) with (27) and (28), hence CDF of $F_{\gamma_B}(\gamma)$ can be obtained as

$$F_{\gamma_B}(\gamma) = \frac{1}{\lambda_1 C_3} + \frac{1}{\lambda_1 C_1}\exp\left(\frac{1}{\lambda_1 C_1}\right)\mathrm{E}_1\left(\frac{1}{\lambda_1 C_1}\right) \times \frac{1}{\lambda_1 C_1}\exp\left(\frac{C_3}{\lambda_1 C_1}\right)\mathrm{E}_1\left(\frac{C_3}{\lambda_1 C_1}\right), \quad (29)$$

where $C_3 \triangleq \frac{\bar{\gamma}\lambda_1(1-\kappa_R^2\gamma)+\omega_1\gamma}{\lambda_1\omega_1\gamma}$. Now we derive the CDF of γ_A as provided in (25). We first notice that $\gamma_{1,BRA}$ and $\gamma_{2,BRA}$ are two mutually independent RVs as shown in (23) and (24), respectively. Thus, the CDF of γ_A can be expressed as

$$F_{\gamma_A}(\gamma) = F_{\gamma_{1,BRA}}(\gamma) + F_{\gamma_{2,BRA}}(\gamma) - F_{\gamma_{1,BRA}}(\gamma)F_{\gamma_{2,BRA}}(\gamma). \quad (30)$$

The CDF of $\gamma_{1,BRA}$ is found based on Proposition 3, while the CDF of $\gamma_{2,BRA}$ is derived with the help of Proposition 2. In particular, we have

$$F_{\gamma_{1,BRA}}(\gamma) = \frac{\gamma\omega_3}{\gamma\omega_3 + \bar{\gamma}\lambda_2(1-\kappa_R^2\gamma)}, \quad (31)$$

$$F_{\gamma_{2,BRA}}(\gamma) = \frac{\omega_2}{\lambda_1^2 C_4}\exp\left(\frac{\omega_2}{\lambda_1^2 C_4}\right)\mathrm{E}_1\left(\frac{\omega_2}{\lambda_1^2 C_4}\right), \quad (32)$$

where $C_4 \triangleq \frac{\bar{\Upsilon}_1(1-\kappa_A^2\gamma)}{\gamma}$. The CDF of γ_A is obtained by inserting (31) and (32) into (30). Consequently, the OP at A and B under the specified SNDR threshold (γ_t) of the network are respectively given in (33)–(34).

$$OP_A(\gamma_t) = \frac{\gamma_t\omega_3}{\gamma_t\omega_3 + \bar{\gamma}\lambda_2(1-\kappa_R^2\gamma_t)} + \frac{\omega_2}{\lambda_1^2 C_4}\exp\left(\frac{\omega_2}{\lambda_1^2 C_4}\right) \times \mathrm{E}_1\left(\frac{\omega_2}{\lambda_1^2 C_4}\right)\left[1 - \frac{\gamma_t\omega_3}{\gamma_t\omega_3 + \bar{\gamma}\lambda_2(1-\kappa_R^2\gamma_t)}\right]. \quad (33)$$

$$OP_B(\gamma_t) = \frac{1}{\lambda_1 C_3} + \frac{1}{\lambda_1 C_1}\exp\left(\frac{1}{\lambda_1 C_1}\right)\mathrm{E}_1\left(\frac{1}{\lambda_1 C_1}\right) \frac{1}{\lambda_1 C_1}\exp\left(\frac{C_3}{\lambda_1 C_1}\right)\mathrm{E}_1\left(\frac{C_3}{\lambda_1 C_1}\right). \quad (34)$$

The OP of TWCR network with SFS policy, TDBC protocol and TSB architecture at a specific SNDR threshold is the sum of the OPs of the link $A \to R \to B$ and the OP of the link $B \to R \to A$, such that

$$OP(\gamma_t) = OP_A(\gamma_t) + OP_B(\gamma_t), \quad (35)$$

where $OP_A(\gamma_t)$ and $OP_B(\gamma_t)$ are the OPs at A and B given in (33) and (34), respectively.

4) THROUGHPUT ANALYSIS

Similar to Section IV-A4, the network throughput with delay limited transmission is obtained as (17) in which $OP_A(\gamma_A)$ and $OP_B(\gamma_B)$ denote the OPs at A and B corresponding to the transmission rate R_A and R_B from (33) and (34).

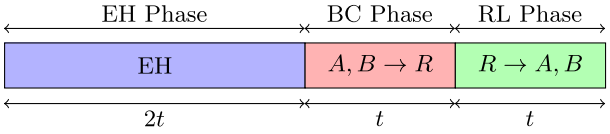

FIGURE 5. Data frame structure of the DS-MABC-TSB network.

C. DS POLICY - MABC PROTOCOL

In this configuration, the network utilizes the DS policy and the MABC protocol while the TSB architecture is implemented in the relay receiver. The data frame structure of the transmission cycle T is shown in Fig. 5. First, R collects energy from transmitted signals from both A and B in the EH phase. Similarly, the harvested energy at R is given as in (3). Then, A and B simultaneously transmit to R in the BC phase. Later, R forwards the received signals to both A and B in the RL phase. In this case, the duration of the BC phase is t [*sec*]. As the transmission rate from A and B is similar to the previous network configuration, therefore, it needs only t [*sec*] to simultaneously transmit data from A and B to R. The duration of T of this configuration is $4t$ [*sec*]. The transmit power at R in the RL phase is parameterized as

$$P_R = \frac{E_H}{2t} = \frac{\mu\widetilde{I}_P 2t}{2t}(\rho_1 + \rho_2) = \Upsilon_2(\rho_1 + \rho_2), \quad (36)$$

where $\Upsilon_2 = \mu\widetilde{I}_P$. As the direct communication link between A and B is not considered in this paper, the SNDRs at A and B in this network configuration are statistically similar to the

SNDRs of the DS-TDBC-TSB networks which derived in Section IV-A. Therefore, the OP of the DS-MABC-TSB networks can be evaluated by following a similar line of reasoning as in Section IV-A with the only difference pertaining to the replacement of $\bar{\Upsilon}_1$ with $\bar{\Upsilon}_2 = \frac{\Upsilon_2}{N_0}$.

Moreover, the throughput the DS-MABC-TSB networks can be calculated as in (17) by appropriate scaling with $\frac{1}{4}$ because the length of one communication cycle of this configuration is $4t$ $[s]$. It is characterized as

$$\mathcal{T} = \frac{1}{4}\Big[R_A(1 - OP_A(\gamma_A)) + R_B(1 - OP_B(\gamma_B))\Big]. \quad (37)$$

D. SFS POLICY - MABC PROTOCOL

In this content, the network is configured with the SFS policy, the MABC protocol while the TSB architecture is implemented in the relay receiver. The data frame structure of the transmission cycle is similar to the one was shown in Fig. 5. However, the relay R only collects energy from the transmitted signal from A in the EH phase. As a result, the transmit power at the relay in the RL phase is expressed as

$$P_R = \frac{E_H}{2t} = \frac{\mu\widetilde{I}_P 2t}{2t}\rho_1 = \Upsilon_2\rho_1. \quad (38)$$

Likewise, the end-to-end SNDRs of the SFS-MABC-TSB networks is statistically similar to those in Section IV-B.2. Thus, we can derive the CDF of the end-to-end SNDRs by (33) and (34) with substituting Υ_2 for Υ_1. In the same manner, we can character the network OP and throughput by the similar method in Section IV-C where $OP_A(\gamma_t)$ and $OP_B(\gamma_t)$ are the OPs at A and B also given in (33) and (34), respectively.

V. PERFORMANCE ANALYSIS: PSB ARCHITECTURE

In this section, the relay receiver is implemented with the PSB architecture. In this PSB receiver architecture, the EH phase and the BC phase occur simultaneously, the relay always harvests energy from the wireless signals that are transmitted from both nodes A and B of the network. Therefore, only the DS energy transfer policy is consider for the network that utilizes the PSB relay receiver structure. We now elaborate the impact of transceiver impairments on the OP and throughput of the EH-TWCR networks with DS policy for different relaying protocols. We note that the power sharing fraction is ε $(0 < \varepsilon < 1)$.

A. DS POLICY - TDBC PROTOCOL

In this configuration, the network utilizes the DS policy and the TDBC protocol. Data frame structure of the transmission cycle is shown in Fig. 6. The relay simultaneously harvests energy and collects data from the wireless signals that are transmitted form A and B consecutively in $2t$ $[s]$ duration. Hence, duration of T is $3t$ $[sec]$. The acquired energy at the relay node is parametrized as

$$E_H = \varepsilon\mu\Big(P_A^{EH}|h_1|^2 + P_B^{EH}|h_2|^2\Big)t = \varepsilon\mu\widetilde{I}_P(\rho_1 + \rho_2)t. \quad (39)$$

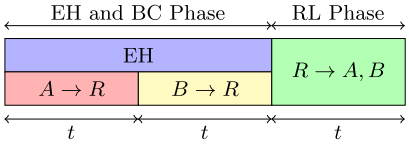

FIGURE 6. Data frame structure of the DS-TDBC-PSB network.

1) TRANSMIT POWER IN THE RL PHASE

The harvested energy is used to power the relay in the current transmission cycle RL phase and the consecutive transmission cycle BC phase. Same as before, we assume that the total harvested energy at R is distributed equally. Thus, from (39), the transmit power in the RL phase equals to

$$P_R = \frac{\varepsilon\mu\widetilde{I}_P(\rho_1 + \rho_2)t}{3t} = \Upsilon_3(\rho_1 + \rho_2), \quad (40)$$

where $\Upsilon_3 = \frac{1}{3}\varepsilon\mu\widetilde{I}_P$.

2) END-TO-END SNDR

Similar to the Section IV-A, only the end-to-end SNDR of the link $A \to R \to B$ will be considered. We assume that A transmits data with the peak power $\frac{I_P}{|g_1|^2}$ in the BC phase, the receiver power of the incoming signal to the data processing block is $(1-\varepsilon)\frac{I_P}{|g_1|^2}$. The SNDR at R of the $A \to R$ wireless link in the first time slot of the BC phase is given by

$$\gamma_1 = \frac{(1-\varepsilon)\frac{I_P}{N_0}|h_1|^2}{(1-\varepsilon)\frac{I_P}{N_0}\kappa_R^2|h_1|^2 + |g_1|^2} = \frac{\hat{\gamma}\rho_1}{\hat{\gamma}\kappa_R^2\rho_1 + \nu_1}, \quad (41)$$

where $\hat{\gamma} = \frac{(1-\varepsilon)I_P}{N_0}$. In the RL phase, R forwards the received data from the previous two time slots to A and B with the transmit power of $\frac{P_R}{|g_2|^2}$, where P_R is given in (40). Then, the SNDR at B of the communication link $R \to B$ is given by

$$\gamma_2 = \frac{\bar{\Upsilon}_3(\rho_1 + \rho_2)}{\bar{\Upsilon}_3\kappa_B^2(\rho_1 + \rho_2) + \frac{\nu_2}{\rho_2}}, \quad (42)$$

where $\bar{\Upsilon}_3 = \frac{\Upsilon_3}{N_0}$. The end-to-end SNDR of the wireless link $A \to R \to B$ of the cognitive DF network with DS energy transfer, TDBC protocol and PSB relay receiver architecture is then given as

$$\gamma = \min(\gamma_1, \gamma_2). \quad (43)$$

3) OUTAGE PERFORMANCE AND THROUGHPUT ANALYSIS

From (41) and (42), it implies that the end-to-end SNDRs of the networks in this case study have identical distribution with the end-to-end SNDRs of the networks in Section IV-A. Hence, the OP of the networks can be characterized as

$$OP(\gamma_t) = OP_A(\gamma_t) + OP_B(\gamma_t), \quad (44)$$

where $OP_A(\gamma_t)$ and $OP_B(\gamma_t)$ are the outage probabilities at A and B, given in (14) and (15), respectively, with the only difference pertaining to the replacement of $\bar{\Upsilon}_1$ with $\bar{\Upsilon}_3$ and $\bar{\gamma}$ with $\hat{\gamma}$. Likewise, the throughput of the networks can be obtained as

$$\mathcal{T} = \frac{1}{3}\big[R_A(1 - OP_A(\gamma_A)) + R_B(1 - OP_B(\gamma_B))\big]. \quad (45)$$

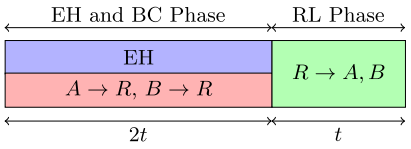

FIGURE 7. Data frame structure of the DS-MABC-PSB network.

B. DS POLICY - MABC PROTOCOL

In this configuration, the network utilizes the DS policy and the MABC protocol. The data frame structure of the transmission cycle is shown in Fig. 7. Due to the assumption that the relay harvests energy from the fix EH duration length, $2t$. Therefore, R simultaneously harvests energy and collects data from the wireless signals that are transmitted in turn form A and B in $2t$ $[s]$ duration. Hence, duration of T is $3t$ $[sec]$. The acquired energy at the relay node is parametrized as

$$E_H = \varepsilon\mu\left(P_A^{EH}|h_1|^2 + P_B^{EH}|h_2|^2\right)2t = \varepsilon\mu\widetilde{I}_P(\rho_1+\rho_2)2t. \tag{46}$$

The harvested energy is used to power the relay in the current transmission cycle RL phase and the BC phase of the next communication cycle. Thus, from (46), the transmit power in the RL phase is given as

$$P_R = \frac{\varepsilon\mu\widetilde{I}_P(\rho_1+\rho_2)2t}{3t} = \Upsilon_4(\rho_1+\rho_2), \tag{47}$$

where $\Upsilon_4 = \frac{2}{3}\varepsilon\mu\widetilde{I}_P$. The OP of the DF TWCR network in this configuration can be evaluated by following a similar line of reasoning as Section IV-A with the only difference pertaining to the replacement of $\bar{\Upsilon}_1$ with $\bar{\Upsilon}_4 = \frac{\Upsilon_4}{N_0}$ and $\bar{\gamma}$ with $\hat{\gamma}$. Moreover, the network throughput of the DS policy, MABC protocol, TSB architecture network can be calculated as in (45).

VI. NUMERICAL RESULTS AND DISCUSSION

In this section, a set of numerical results for the OP and throughput of the DF TWCR networks with different energy transfer policies, relaying protocols and receiver architectures are presented. The network nodes are arranged in Cartesian coordinates where node A is located at the origin. We consider the case where coordinates of relay R, node B and Rx are $(0.4, 0)$, $(1, 0)$ and $(0.8, 0.8)$, respectively. The relation between transmitted and received power with distance d is given by the decaying path loss model d^{-2}. The fixed transmission rates R_A and R_B are chosen to be 2 [bits/s/Hz] to acquire the OP and delay-limited network throughput. Furthermore, the hardware impairment in the range $[0, 0.175]$ are examined, which resemble the maximum tolerable error vector magnitudes (EVMs) of 3GPP LTE requirements. For the sake of clarity, we assume that $\kappa_A^2 = \kappa_B^2 = \kappa_R^2 = \kappa^2$, the energy conversion efficiency is taken as $\mu = 0.8$ and the power sharing fraction is set to $\varepsilon = 0.5$, unless otherwise stated. We note that all the equation in this paper are also applicable for the ideal transceiver, $\kappa^2 = 0$.

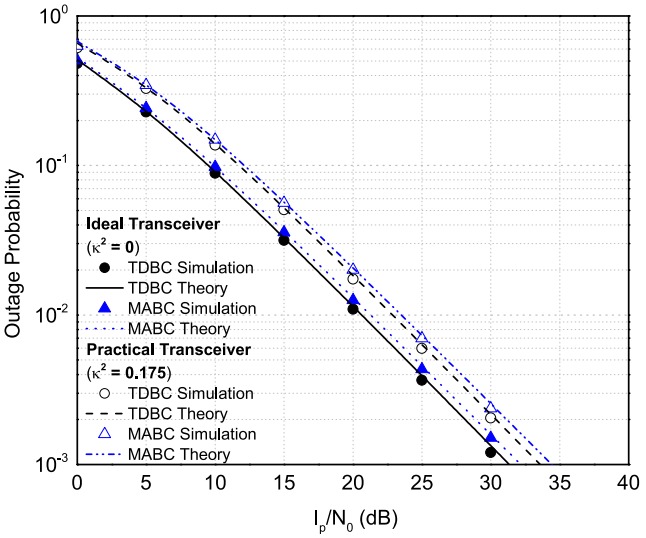

FIGURE 8. OP at A (or at B) of DS-TSB network with respect to I_P/N_0.

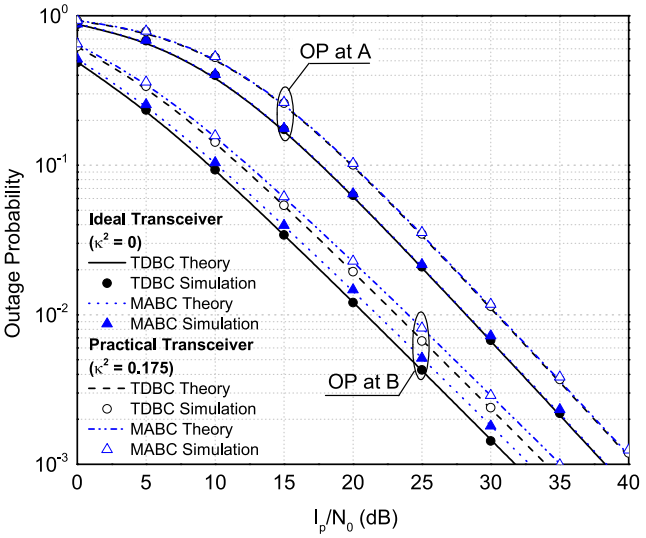

FIGURE 9. OP at A of SFS-TSB network with respect to I_P/N_0.

A. CORROBORATION OF ANALYTICAL OP RESULTS

In this subsection, the analysis results of network OP and throughput provided in Section IV and V are verified. First, the analytical results of the OP in the network with TSB relay receiver architecture are plotted. Fig. 8–9 respectively show the OP at A and B node of the DF TWCR networks with TSB receiver architecture with respect to $\frac{I_P}{N_0} \in [0, 40]$ (dB). It can be seen that the analysis and simulation results are identical in all cases of the TSB network when different energy transfer policies and relaying protocols are employed. Accordingly, our analysis of OP at node A and B as given in (14), (15), (33) and (34) are verified. As anticipated, the OP at A and B in the DS energy transfer policy are similar for the same transmission protocol while the OP at A in the SFS energy transfer policy is much higher compared to the OP at B; in fact, the OP at A is higher than the OP at B due to the difference of distribution in two random variables

$\gamma_{2,ARB}$ and $\gamma_{2,BRA}$. This indicates that the node chosen to transfer energy to the relay has the highest OP. Impact of transceiver imperfections is clearly shown by the increment of OP when the ideal transceiver ($\kappa^2 = 0$) is replaced by the impairment transceiver ($\kappa^2 = 0.175$).

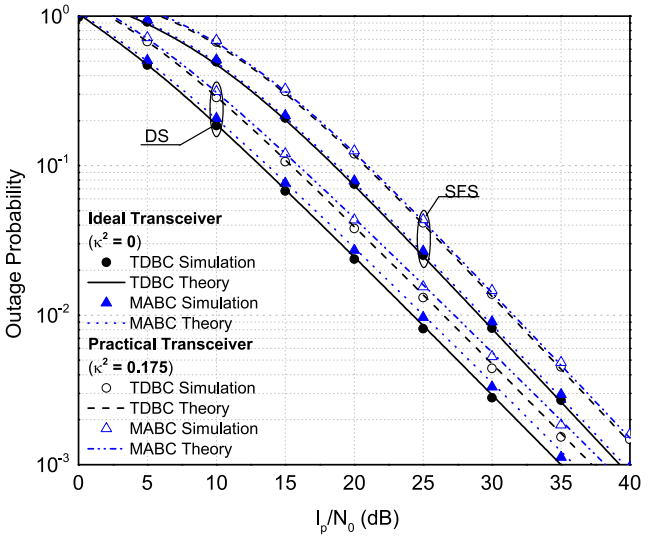

FIGURE 10. TSB network OP with respect to I_P/N_0.

Fig. 10 illustrates the OP of EH-TWCR network with respect to $\frac{I_P}{N_0} \in [0, 40]$ (dB) where the relay utilizes TSB receiver architecture. As shown in the figure, network OP in analysis and simulation of the TSB relay receiver network match for all possible cases of energy transfer policies and relaying protocols under either ideal ($\kappa^2 = 0$) or impairment transceiver ($\kappa^2 = 0.175$). With the same level of hardware impairments, the DS-TDBC network achieves the best OP performance whereas the SFS-MABC network provides the worst among four networks configurations. More specifically, the networks with DS policy outperform the networks with SFS policy. This can be explained by the fact that transmit power in DS policy is higher than in SFS policy. We also observe that the TDBC networks provides the OP less than the network with MABC in term of OP due to the benefit of serial transmission in the TDBC protocol. When we consider the impact of transceiver impairment, we experience an approximate 2.5 dB loss in the SNR while maintaining the OP at nodes A and B when the impairment level κ^2 increases from 0 to 0.175 for the TSB network with all scenarios of energy transfer policies and relaying protocols.

The corroboration of OP analytical results of the PSB network with the SFS energy transfer policy and the TDBC/MABC relaying protocol can be obtained similarly. However, those results are not be plotted to avoid duplication and to maintain the clarity.

B. ACHIEVED THROUGHPUT

Fig. 11 illustrates throughput of the DF TWCR network with respect to $\frac{I_P}{N_0} \in [0, 40]$ (dB) for six configurations of

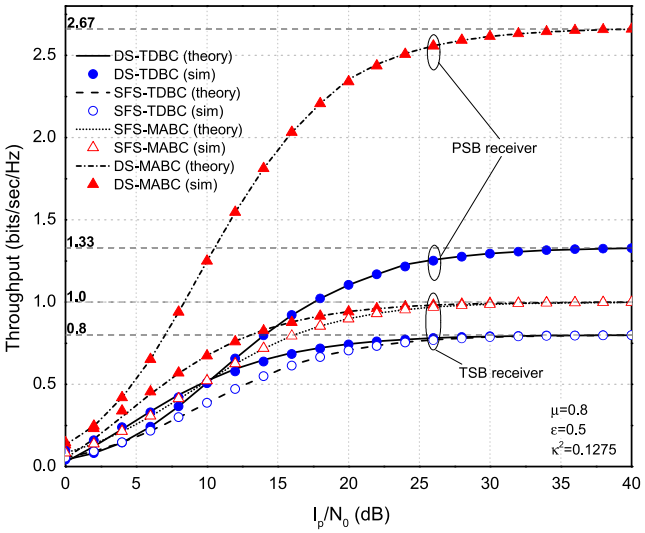

FIGURE 11. Throughput respect to policies, protocols and receiver architecture.

the networks with different energy transfer policies, relaying protocols and relay receiver structures that are considered in this work. The obtained results corresponding to the specific hardware impairment level, $\kappa^2 = 0.1275$. It can be seen that the DS-MABC-PSB networks is offered highest throughput among all other network configurations. On the other end, the SFS-TDBC-TSB networks provides the smallest throughput. This phenomenon can be attributed to the fact that DS policy provides more energy to transmit data in the RL phase than the SFS policy, and also the transmission cycle in the MABC-PSB network is the shortest whereas it is the longest in TDBC-TSB network. The networks utilizes MABC protocol and PSB receiver architecture outperform the TDBC-TSB networks in term of throughput because the benefit of data frame structure duration. However, MABC relaying protocol is more sophisticated to implement since the relay receives signals from A and B in one time slot.

Interestingly, the MABC-PSB network can achieve throughput higher than the transmission rate of each source node while the network with other combinations of relaying protocols and receiver architecture can only provide throughput less than the transmission rate of each source node. In the low SNR regime, $\frac{I_P}{N_0} < 10$ [dB], throughput of the DS-TDBC-PSB networks outperform only the SFS-TDBC-TSB networks. In the high $\frac{I_P}{N_0} > 35$ [dB] regime where system OP approaches to zero, the ceiling throughputs of each combined policies, protocols, and receiver architecture are established. In our simulation scenario with the fixed transmission rate $R_A = R_B = 2$ [bits/s/Hz], the ceiling throughput of the MABC-PSB network and the TDBC-TSB networks are 2.67 and 0.8 [bits/s/Hz], respectively. This fact can be explained by the advantages of transmit power and the length of transmission data frame as above and a notation of the reception rate at the relay is sum of the transmission rate of two source nodes.

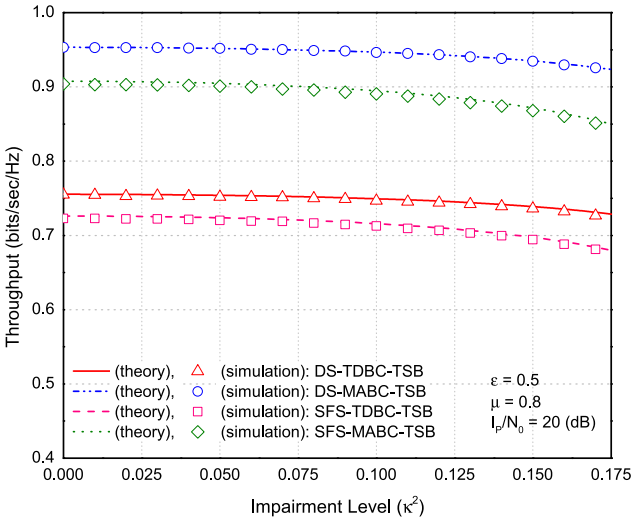

FIGURE 12. Throughput with respect to κ^2 for the TSB receiver.

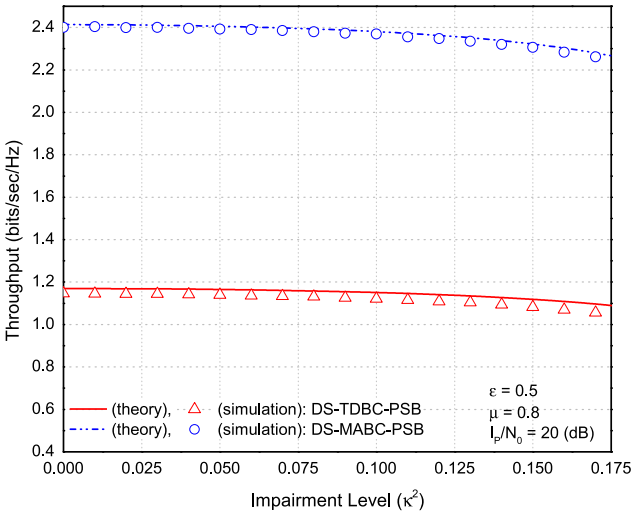

FIGURE 13. Throughput with respect to κ^2 for the PSB receiver.

C. THE IMPACT OF TRANSCEIVER IMPAIRMENTS (κ^2)

Fig. 12 illustrates the throughput of network with respects to hardware impairment levels, $\kappa^2 \in [0, 0.175]$. As shown in Fig. 12, the throughput decreases as κ^2 increases from 0 to 0.18 for the network with TSB receiver structure. This trend is observed for the networks with all possible configurations. In the context of delay limit transmission, the decrement in throughput for the network with MABC protocol is more noticeable than the network with TDBC protocol. The impact of hardware impairment on throughput of network with the SFS policy is more remarkable than the network with DS policy. These observations suggest that the network utilizing MABC protocol or the SFS policy is more sensitive to transceiver' quality than the TDBC protocol or the DS policy. Therefore, the combination of DS policy and TDBC protocol for the EH-TWCR network provides the highest level of limiting factor impact of transceiver hardware impairment on the network throughput. A similar conclusion is made for the throughput of network with PSB relay receiver structure as in Fig. 13.

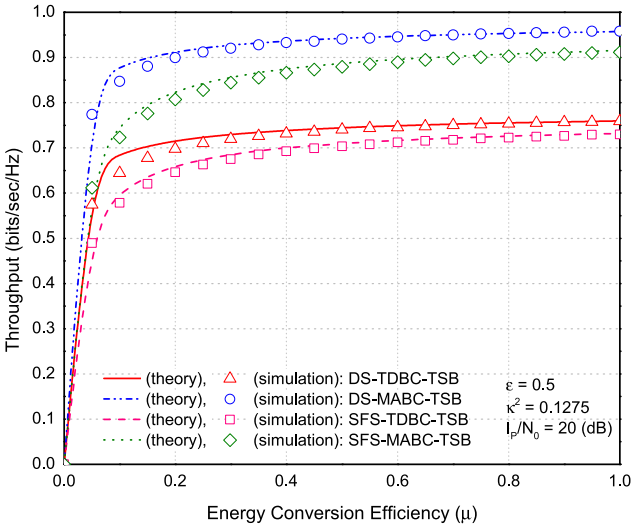

FIGURE 14. Throughput with respect to μ for the TSB receiver.

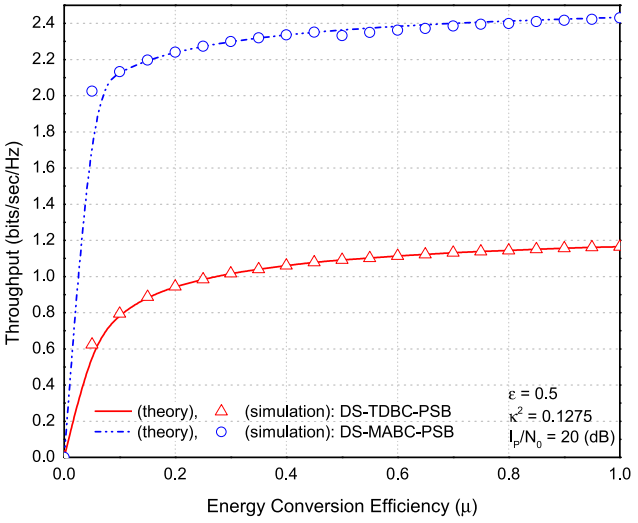

FIGURE 15. Throughput with respect to μ for the PSB receiver.

D. THE EFFECT OF ENERGY CONVERSION EFFICIENCY (μ)

Fig. 14–15 illustrate the delay limit throughput respects to the energy conversion efficiency, $\mu \in [0, 1]$ for different network configurations. It can be seen that the throughput increases from 0 to ceiling throughput as μ increases from 0 to 1 for all cases. The throughput of SFS networks approaches to the ceiling throughput as μ increases slower than the network with DS protocol. This is because the transmit power in the RL phase of the SFS networks is smaller than that of the DS networks, therefore the low quality EH circuitry impact the throughput of networks with the SFS policy more than the networks with DS policy.

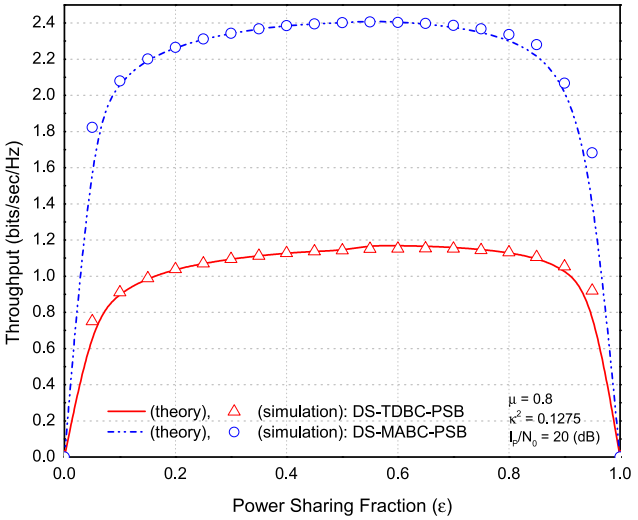

FIGURE 16. Throughput with respect to ε for the PSB receiver architecture.

E. THE EFFECT OF POWER SHARING FACTOR (ε)

Fig. 16 shows the effect of power sharing factor ε to the network throughput of the PSB network. The throughput increase as ε rises from 0 to the optimal value of ε, but it decreases as ε increases from the optimal value to 1. It can be explained based on the harvested power in the EH phase and the power of received signal in the BC phase. When ε is smaller than the optimal value, the harvested power increase while the received signal power is decreased as ε increases. The received signal powers at the data processing block still higher than the level that is required to decode the signal correctly. Thus, the network throughput increases. However, when ε is larger than the optimum value, the harvested energy still increases but the power of incoming signal to the data processing is lower than the required level, hence, the transmit signal is recovered improperly at the relay. Eventually, the throughput of the network decreases.

VII. CONCLUSION

This paper investigated outage probability and throughput of a EH-TWCR network. Our analysis provided a insight into a practical self-powered TWCR network based on DF. For instance, it was found that the DS-MABC-PSB provides the best throughput among our considered configuration albeit at the expense of complexity. Whereas, the SFS-TDBC-TSB network offers a simpler implementation with a lower throughput. In principle, a network with the SFS policy and MABC protocol is more sensitive to hardware impairments than those with DS policy and TDBC protocol. We also confirmed that the transceiver impairments substantially deteriorate network' outage probability and throughput. As presented, system performance degradation caused by transceiver imperfection can be quantified as a function of hardware impairment level. This interesting result can be used to select hardwares for the EH-TWCR network at an appropriate quality that meets the predetermined outage probability and throughput.

REFERENCES

[1] J. A. Paradiso and T. Starner, "Energy scavenging for mobile and wireless electronics," *IEEE Pervasive Comput.*, vol. 4, no. 1, pp. 18–27, Jan./Mar. 2005.
[2] V. Raghunathan, S. Ganeriwal, and M. Srivastava, "Emerging techniques for long lived wireless sensor networks," *IEEE Commun. Mag.*, vol. 44, no. 4, pp. 108–114, Apr. 2006.
[3] T. Le, K. Mayaram, and T. Fiez, "Efficient far-field radio frequency energy harvesting for passively powered sensor networks," *IEEE J. Solid-State Circuits*, vol. 43, no. 5, pp. 1287–1302, May 2008.
[4] Y.-H. Suh and K. Chang, "A high-efficiency dual-frequency rectenna for 2.45- and 5.8-GHz wireless power transmission," *IEEE Trans. Microw. Theory Techn.*, vol. 50, no. 7, pp. 1784–1789, Jul. 2002.
[5] J. R. Smith, *Wirelessly Powered Sensor Networks and Computational RFID*. New York, NY, USA: Springer, 2013.
[6] K. Huang and V. K. N. Lau, "Enabling wireless power transfer in cellular networks: Architecture, modeling and deployment," *IEEE Trans. Wireless Commun.*, vol. 13, no. 2, pp. 902–912, Feb. 2014.
[7] S. Maleki, G. Leus, S. Chatzinotas, and B. Ottersten, "To AND or to OR: On energy-efficient distributed spectrum sensing with combined censoring and sleeping," *IEEE Trans. Wireless Commun.*, vol. 14, no. 8, pp. 4508–4521, Aug. 2015.
[8] L. Yang, M. S. Alouini, and K. Qaraqe, "On the performance of spectrum sharing systems with two-way relaying and multiuser diversity," *IEEE Commun. Lett.*, vol. 16, no. 8, pp. 1240–1243, Aug. 2012.
[9] K. J. Kim, T. Q. Duong, M. Elkashlan, P. L. Yeoh, and A. Nallanathan, "Two-way cognitive relay networks with multiple licensed users," in *Proc. IEEE GLOBECOM*, Dec. 2013, pp. 992–997.
[10] Y. Zou, M. Valkama, and M. Renfors, "Digital compensation of I/Q imbalance effects in space-time coded transmit diversity systems," *IEEE Trans. Signal Process.*, vol. 56, no. 6, pp. 2496–2508, Jun. 2008.
[11] J. Qi, S. Aïssa, and M.-S. Alouini, "Analysis and compensation of I/Q imbalance in amplify-and-forward cooperative systems," in *Proc. IEEE WCNC*, Apr. 2012, pp. 215–220.
[12] J. Li, M. Matthaiou, and T. Svensson, "I/Q imbalance in two-way AF relaying," *IEEE Trans. Commun.*, vol. 62, no. 7, pp. 2271–2285, Jul. 2014.
[13] J. Qi and S. Aïssa, "On the power amplifier nonlinearity in MIMO transmit beamforming systems," *IEEE Trans. Commun.*, vol. 60, no. 3, pp. 876–887, Mar. 2012.
[14] A. K. Papazafeiropoulos, S. K. Sharma, and S. Chatzinotas, "MMSE filtering performance of DH-AF massive MIMO relay systems with residual transceiver impairments," in *Proc. IEEE Int. Conf. Commun.*, Kuala Lumpur, Malaysia, May 2016, pp. 644–649.
[15] A. K. Papazafeiropoulos, S. K. Sharma, and S. Chatzinotas, "Impact of transceiver impairments on the capacity of dual-hop relay massive MIMO systems," in *Proc. IEEE GLOBECOM*, San Diego, CA, USA, Dec. 2015, pp. 1–6.
[16] E. Björnson, M. Matthaiou, and M. Debbah, "A new look at dual-hop relaying: Performance limits with hardware impairments," *IEEE Trans. Commun.*, vol. 61, no. 11, pp. 4512–4525, Nov. 2013.
[17] T. M. Cover and A. A. El Gamal, "Capacity theorems for the relay channel," *IEEE Trans. Inf. Theory*, vol. 25, no. 5, pp. 572–584, Sep. 1979.
[18] K. B. Letaief and W. Zhang, "Cooperative communications for cognitive radio networks," *Proc. IEEE*, vol. 97, no. 5, pp. 878–893, May 2009.
[19] T. E. Hunter, S. Sanayei, and A. Nosratinia, "Outage analysis of coded cooperation," *IEEE Trans. Inf. Theory*, vol. 52, no. 2, pp. 375–391, Feb. 2006.
[20] A. A. Nasir, X. Zhou, S. Durrani, and R. A. Kennedy, "Relaying protocols for wireless energy harvesting and information processing," *IEEE Trans. Wireless Commun.*, vol. 12, no. 7, pp. 3622–3636, Jul. 2013.
[21] B. Medepally and N. B. Mehta, "Voluntary energy harvesting relays and selection in cooperative wireless networks," *IEEE Trans. Wireless Commun.*, vol. 9, no. 11, pp. 3543–3553, Nov. 2010.
[22] T. Schenk, *RF Imperfections in High-Rate Wireless Systems: Impact and Digital Compensation*. New York, NY, USA: Springer, 2010.
[23] M. Matthaiou, A. Papadogiannis, E. Björnson, and M. Debbah, "Two-way relaying under the presence of relay transceiver hardware impairments," *IEEE Commun. Lett.*, vol. 17, no. 6, pp. 1136–1139, Jun. 2013.
[24] D. K. Nguyen, M. Matthaiou, T. Q. Duong, and H. Ochi, "RF energy harvesting two-way cognitive DF relaying with transceiver impairments," in *Proc. IEEE Commun. Workshop (ICCW)*, Jun. 2015, pp. 1970–1975.

[25] X. Zhou, R. Zhang, and C. K. Ho, "Wireless information and power transfer: Architecture design and rate-energy tradeoff," in *Proc. IEEE GLOBECOM*, Dec. 2012, pp. 3982–3987.
[26] E. Björnson, P. Zetterberg, and M. Bengtsson, "Optimal coordinated beamforming in the multicell downlink with transceiver impairments," in *Proc. IEEE GLOBECOM*, Dec. 2012, pp. 4775–4780.
[27] N. Zhao, F. R. Yu, and V. C. M. Leung, "Opportunistic communications in interference alignment networks with wireless power transfer," *IEEE Wireless Commun.*, vol. 22, no. 1, pp. 88–95, Feb. 2015.
[28] N. Zhao, F. R. Yu, H. Sun, and M. Li, "Adaptive power allocation schemes for spectrum sharing in interference-alignment-based cognitive radio networks," *IEEE Trans. Veh. Technol.*, vol. 65, no. 5, pp. 3700–3714, May 2016.
[29] N. Zhao, F. R. Yu, and V. C. M. Leung, "Wireless energy harvesting in interference alignment networks," *IEEE Commun. Mag.*, vol. 53, no. 6, pp. 72–78, Jun. 2015.
[30] Q. Wu, W. Chen, and J. Li, "Wireless powered communications with initial energy: QoS guaranteed energy-efficient resource allocation," *IEEE Commun. Lett.*, vol. 19, no. 12, pp. 2278–2281, Dec. 2015.
[31] Q. Wu, W. Chen, D. W. K. Ng, J. Li, and R. Schober, "User-centric energy efficiency maximization for wireless powered communications," *IEEE Trans. Wireless Commun.*, vol. 15, no. 10, pp. 6898–6912, Oct. 2016.
[32] Q. Wu, M. Tao, D. W. K. Ng, W. Chen, and R. Schober, "Energy-efficient resource allocation for wireless powered communication networks," *IEEE Trans. Wireless Commun.*, vol. 15, no. 3, pp. 2312–2327, Mar. 2016.
[33] Z. Chang *et al.*, "Energy efficient resource allocation for wireless power transfer enabled collaborative mobile clouds," *IEEE J. Sel. Areas Commun.*, vol. 34, no. 12, pp. 3438–3450, Dec. 2016, doi: 10.1109/JSAC.2016.2611843.
[34] Z. Chang, J. Gong, T. Ristaniemi, and Z. Niu, "Energy-efficient resource allocation and user scheduling for collaborative mobile clouds with hybrid receivers," *IEEE Trans. Veh. Technol.*, vol. 65, no. 12, pp. 9834–9846, Dec. 2016.
[35] Z. Chang, Q. Zhang, X. Guo, and T. Ristaniemi, "Energy-efficient resource allocation for OFDMA two-way relay networks with imperfect CSI," *EURASIP J. Wireless Commun. Netw.*, vol. 2015, no. 1, p. 225, Oct. 2015.
[36] S. Luo, R. Zhang, and T. J. Lim, "Optimal save-then-transmit protocol for energy harvesting wireless transmitters," *IEEE Trans. Wireless Commun.*, vol. 12, no. 3, pp. 1196–1207, Mar. 2013.
[37] S. Gollakota, M. S. Reynolds, J. R. Smith, and D. J. Wetherall, "The emergence of RF-powered computing," *Computer*, vol. 47, no. 1, pp. 32–39, Jan. 2014.
[38] I. Gradshteyn and I. Ryzhik, *Table of Integrals, Series, and Products*, 6th ed. New York, NY, USA: Academic, 2000.
[39] Y. Guo, G. Kang, N. Zhang, W. Zhou, and P. Zhang, "Outage performance of relay-assisted cognitive-radio system under spectrum-sharing constraints," *Electron. Lett.*, vol. 46, no. 2, pp. 182–184, Jan. 2010.
[40] C. Zhong, T. Ratnarajah, and K.-K. Wong, "Outage analysis of decode-and-forward cognitive dual-hop systems with the interference constraint in Nakagami-*m* fading channels," *IEEE Trans. Veh. Technol.*, vol. 60, no. 6, pp. 2875–2879, Jul. 2011.

DANG KHOA NUYEN received the B.E. degree in electronics and telecommunication from the University of Technology, Ho Chi Minh, Vietnam, in 2008, the M.S. degree in electronics and telecommunication from the University of Science, Ho Chi Minh, Vietnam, in 2012, and the Ph.D degree in Information System from the Kyushu Institute of Technology, Japan, in 2016. He has joined the Wireless Communication Networks Laboratory, Aalborg University, Denmark, as an Industrial Post-Doctoral Researcher from 2016. His research interests are cognitive networks, relay networks, and wireless signal processing.

DUSHANTHA NALIN K. JAYAKODY (M'14) received the B. E. electronics engineering degree (Hons.) from Pakistan in 2009 under SAARC Scholarship, the M.Sc. degree (Hons.) in electronics and communications engineering from the Department of Electrical and Electronics Engineering, Eastern Mediterranean University, Turkey, in 2010, under the University Full Graduate Scholarship, and the Ph. D. degree in electronics, electrical, and communications engineering from the University College Dublin, Ireland, in 2014. From 2014 to 2016, he has held a post-doctoral position with the Coding and Information Transmission Group, University of Tartu, Estonia, and with the University of Bergen, Norway. Since 2016, he is a Professor with the Department of Software Engineering, Institute of Cybernetics, National Research Tomsk Polytechnic University, Russia. He has served as Session Chair or Technical Program Committee Member for various international conferences, such as the IEEE PIMRC, the IEEE WCNC, the IEEE VTC in 2015.

SYMEON CHATZINOTAS (S'06–M'09–SM'13) received the M.Eng. degree in telecommunications from the Aristotle University of Thessaloniki, Thessaloniki, Greece, and the M.Sc. and Ph.D. degrees in electronic engineering from the University of Surrey, Surrey, U.K., in 2003, 2006, and 2009, respectively. He has worked on numerous RD projects for the Institute of Informatics Telecommunications, National Center for Scientific Research Demokritos, Institute of Telematics and Informatics, Center of Research and Technology Hellas, and Mobile Communications Research Group, Center of Communication Systems Research, University of Surrey, Surrey, U.K. He is currently a Research Scientist with the SIGCOM Research Group, Interdisciplinary Centre for Security, Reliability, and Trust, University of Luxembourg, Luxembourg, where he is involved in managing the H2020, ESA, and FNR projects. He has authored over 120 technical papers in refereed international journals, conferences, and scientific books. His research interests include multiuser information theory, co-operative/cognitive communications, and wireless networks optimization. He was a co-recipient of the 2014 Distinguished Contributions to Satellite Communications Award, and the Satellite and Space Communications Technical Committee, the IEEE Communications Society, and the CROWNCOM 2015 Best Paper Award. He is one of the editors of the book *Cooperative and Cognitive Satellite Systems* (Elsevier, 2015) and was involved in co-organizing the First International Workshop on Cognitive Radios and Networks for Spectrum Coexistence of Satellite and Terrestrial Systems in conjunction with the IEEE ICC 2015, London, U.K., in 2015.

JOHN S. THOMPSON (SM'13–F'16) received the B.Eng. and Ph.D. degrees from the University of Edinburgh, Edinburgh, U.K., in 1992 and 1996, respectively. He currently holds a Personal Chair in signal processing and communications with the School of Engineering, University of Edinburgh, Edinburgh, U.K. His current research interests include antenna array processing, cooperative communications systems, and energy-efficient wireless communications. His work in these areas is highly cited. He is a Distinguished Lecturer for the IEEE Communications Society for 2014–2015. He was the Lead Editor of the *IEEE Communications Magazine* Special Issue on 5G Wireless Communication Systems: Prospects and Challenges, published in 2014. He was an elected member for the Board of Governors of the IEEE Communications Society from 2012 to 2014. He is also serving as a Tutorial Co-Chair for the 2015 IEEE International Conference on Communications, London, U.K. His h-index is currently 21 according to Web of Science.

JUN LI (M'09–SM'16) received the Ph.D. degree in electronic engineering from Shanghai Jiao Tong University, Shanghai, China, in 2009. In 2009, he was with the Department of Research and Innovation, Alcatel Lucent Shanghai Bell, as a Research Scientist. From 2009 to 2012, he was a Post-Doctoral Fellow with the School of Electrical Engineering and Telecommunications, University of New South Wales, Australia. From 2012 to 2015, he was a Research Fellow with the School of Electrical Engineering, University of Sydney, Australia. Since 2015, he has been a Professor with the School of Electronic and Optical Engineering, Nanjing University of Science and Technology, Nanjing, China. His research interests include network information theory, channel coding theory, wireless network coding, and resource allocations in cellular networks.